J. Biochem. **141,** 411–420 (2007)
doi:10.1093/jb/mvm045

Biophysics and Bioinformatics Reveal Structural Differences of the Two Peripheral Stalk Subunits in Chloroplast ATP Synthase

Ansgar Poetsch[1,†], Richard J. Berzborn[1], Joachim Heberle[2,*], Thomas A. Link[3], Norbert A. Dencher[4] and Holger Seelert[4,‡]

[1]Lehrstuhl für Biochemie der Pflanzen, Ruhr-Universität Bochum, Universitätsstr. 150, D-44801 Bochum, Germany; [2]Forschungszentrum Jülich, IBI-2: Structural Biology, D-52425 Jülich, Germany; [3]Institute of Biophysics, J. W. von Goethe-Universität, Theodor-Stern-Kai 7, D-60590 Frankfurt/Main, Germany; and [4]Department of Chemistry, Physical Biochemistry, Darmstadt University of Technology, Petersenstrasse 22, D-64287 Darmstadt, Germany

Received November 2, 2006; accepted January 17, 2007; published online February 5, 2007

ATP synthases convert an electrochemical proton gradient into rotational movement to produce the ubiquitous energy currency adenosine triphosphate. Tension generated by the rotational torque is compensated by the stator. For this task, a peripheral stalk flexibly fixes the hydrophilic catalytic part F_1 to the membrane integral proton conducting part F_O of the ATP synthase. While in eubacteria a homodimer of b subunits forms the peripheral stalk, plant chloroplasts and cyanobacteria possess a heterodimer of subunits I and II. To better understand the functional and structural consequences of this unique feature of photosynthetic ATP synthases, a procedure was developed to purify subunit I from spinach chloroplasts. The secondary structure of subunit I, which is not homologous to bacterial b subunits, was compared to heterologously expressed subunit II using CD and FTIR spectroscopy. The content of α-helix was determined by CD spectroscopy to 67% for subunit I and 41% for subunit II. In addition, bioinformatics was applied to predict the secondary structure of the two subunits and the location of the putative coiled–coil dimerization regions. Three helical domains were predicted for subunit I and only two uninterrupted domains for the shorter subunit II. The predicted length of coiled–coil regions varied between different species and between subunits I and II.

Key words: bioinformatics, CD spectroscopy, dimerization, F_OF_1, FTIR.

Abbreviations: CD, circular dichroism; CF_OF_1, proton translocating ATP synthase of chloroplasts; CHAPS, 3-[(cholamidopropyl)dimethylammonio]-propanesulfonate; DTT, dithiothreitol; F_1, hydrophilic part of ATP synthase; F_O, hydrophobic, membrane integral part of ATP synthase.

The ATP synthase, the enzyme responsible for the generation of the bulk of the ubiquitous energy currency adenosine triphosphate (ATP) in all living organisms, represents the smallest rotary motor in nature. This machinery consists of a hydrophilic portion F_1 (subunit composition: $\alpha_3\beta_3\gamma\delta\varepsilon$) catalysing the synthesis of ATP and a membrane integral portion F_O (in chloroplast: I, II, III_{14}, IV) responsible for the conversion of an electrochemical proton gradient into rotational motion. In mitochondrial ATP synthases, accessory subunits are present. Two thin stalks join F_O and F_1, which was clearly shown by cryoelectron microscopy [e.g. Böttcher *et al*. (*1*) for chloroplast ATP synthase]. The rotating central stalk in the ATP synthase is composed of subunits γ and ε. A second stalk, consisting of subunits I, II and δ in chloroplasts and connecting F_1 and F_O at the periphery, stabilizes the rotating machinery as a stator.

While F_1 has been characterized structurally and functionally in detail, the knowledge about F_O is only poor. The problems in handling of membrane integral proteins and instability of protein complexes lead to the absence of high-resolution X-ray or electron crystallographic structures including the entire F_O subunits. The structure of a subcomplex F_1c_{10} without the other F_O subunits could be obtained for the yeast enzyme at 3.9 Å resolution (*2*). Isolated cylindrical oligomers are characterized by high-resolution X-ray crystallography of the Na^+-translocating ATP synthase from *Ilyobacter tartaricus* (*3*) and of the V-type Na^+-ATPase from *Enterococcus hirae* (*4*). The topography and stoichiometry of the III oligomer was determined by atomic force microscopy for the ATP synthase from spinach chloroplasts (*5*) and *I. tartaricus* (*6*). While in *Escherichia coli* the secondary structure of subunit c was solved by NMR (*7*), the secondary structure or the topography of the chloroplast F_O subunits are uncertain. So far, only very little structural and biochemical knowledge about the subunits I and II from chloroplasts is available.

To accomplish its task as a link between the subunits residing in the membrane to the distant surface exposed subunits α and β, the peripheral stalk has to be both a stable and a flexible connection. While δ is supposed to be

*Present address: University Bielefeld, Biophysical Chemistry PC III, D-33501 Bielefeld
†To whom correspondence should be addressed. Tel: +49-234-32-24535, Fax: +49-234-32-14322,
E-mail: ansgar.poetsch@ruhr-uni-bochum.de
‡Correspondence may also be addressed: Tel: +49-6151-16-5193, Fax: +49-6151-16-4171, E-mail: seelert@hrzpub.tu-darmstadt.de

located on top of F_1 (*8*), subunits I and II in chloroplast are responsible for the F_O–F_1 connection. In bacteria the homologous structural elements constitute a dimer of b subunits (*9*, *10*). To stabilize the dimer and ultimately the complete ATP synthase, coiled–coil interactions have been described for subunit b in eubacteria and mitochondria (*11*, *12*). For the chloroplast subunits I and II similar interactions can also be expected, but no report has been published so far. The sequence of *E. coli* b has been divided into four domains (membrane-integral, tether, dimerization and δ-binding domain) (*13*). In mitochondria only one copy of a b-homologue is present, interacting with an assembly of other subunits (*14*). Most probably, the presence of two different subunits in chloroplast and cyanobacteria can be attributed to a gene duplication. For cyanobacteria, dimerization of the different subunits b and b′ (I and II in chloroplasts) was shown to be very specific (*15*). A 10–20% increase in α-helical content in the b + b′ dimer in comparison to the single subunits indicates structural flexibility of the isolated subunits. A comparable study of the homologous subunits I and II in chloroplasts is lacking.

Two different structural domains (a membrane integral and a hydrophilic part) were predicted for subunits I and II (*16*). In *E. coli* the membrane part and the hydrophilic part of the b subunit [homologous to chloroplast II, but not to I (*17*)] were expressed and examined separately. Only one helix is anchoring the b subunit in the membrane, this domain was characterized with NMR spectroscopy (*18*). Additionally, the crystal structure of the dimerization domain for a single b subunit was solved (*12*). However, since the domain did not crystallize as a dimer, the solved structure probably does not reflect the conformation of b in the ATP synthase complex. Subunit b should be very flexible to allow a connection of F_1 and F_O over a distance of 110 Å (*19–21*); without loss of function, 7–14 amino acids can be added or 7–11 amino acids removed in the region between Ala-50 and Ile-75 in the *E. coli* subunit b (*22*, *23*). Moreover, b subunits of unequal lengths were tolerated in the ATP synthase (*24*).

In the present work we describe the first isolation method for pure subunit I. CD and FTIR spectroscopy indicated that subunit I is predominantly α-helical and that the secondary structures of subunits I and II differ significantly. Dimerization domains of different lengths are predicted for subunits I and II. Sequence analysis predicts three helical segments for subunit I but only two segments for subunit II.

MATERIALS AND METHODS

Bioinformatics—Protein sequences were retrieved using protein–protein BLAST (version 2.2.6) (*25*) searches with default parameters on the nr database (released May 3, 2003). The sequences of the subunits I and II from spinach were used as input. The sequence of subunit II from *C. reinhardtii* was retrieved from ChlamyDB. For the bioinformatic analysis sequences were applied as provided by the databases (which means both, spinach and *C. reinhardtii* subunit II, include transition peptide sequences). Coiled–coil regions were predicted with the programs Coils (window size 21, matrix MTIDK, no position weighting) (*26*), Paircoil (*27*), and Marcoil (*28*). Secondary structure of the mature subunits I and II (*17*) was predicted with the programs PHD (both single-sequence and multiple-sequence-alignment-based prediction) (*29*), SamT-02 (*30*), SSpro (*31*) and PSIPRED (*32*).

Isolation of CF_OF_1—Spinach CF_OF_1 was isolated by a modified procedure (*33*) of Pick and Racker (*34*) employing rate-zonal centrifugation as last purification step. ATP synthase was collected from the sucrose step gradient in 30 mM Tris, 30 mM succinate/NaOH pH 6.5, 0.5 mM EDTA, 1 mg/ml asolectin and about 30% sucrose, in the presence of either 0.2% Triton X-100 or 12 mM 3-[(cholamidopropyl)dimethylammonio]-propanesulfonate (CHAPS) as detergent.

Isolation of Subunit I—Forty milligrams CF_OF_1 from the sucrose gradient with Triton X-100 or CHAPS as detergent (6–8 ml) were dialysed against 1 l buffer A [10 mM Tricine/NaOH pH 7.8, 5 mM dithiothreitol (DTT)] for 12 h at 4°C using a visking type 8 (Biomol International L.P., Plymouth Meeting, PA, USA) dialysis tubing with a cut-off of 12 kDa. If subunit I should be examined by UV spectroscopy, CF_OF_1 from the sucrose gradient with CHAPS (Calbiochem, La Jolla, CA, USA) as detergent was used, and 0.2% (w/v) hydrogenated Triton X-100 (Calbiochem, La Jolla, CA, USA) was added to the sample before dialysis. A DEAE–Trisacryl M (Biosepra, Villeneuve la Garenne Cedex, France) column ($h = 20$ cm, $d = 5$ cm) was equilibrated with 120 ml buffer A at a flow rate of 1 ml/min using a Kontron 422 HPLC pump (Kontron Instruments, Milan, Italy) the day before chromatography of CF_OF_1. The dialyzed ATP synthase was applied on the column at a flow rate of 2 ml/min and absorbance at 280 nm in the range 0–0.2 was monitored with a Kontron 332 UV-Vis detector (Kontron Instruments, Milan, Italy). The chromatography at a flow rate of 1 ml/min was performed with buffers in the following order: 60 ml buffer A, 120 ml buffer B [buffer A + 20 mM Zwittergent 3–12 (Calbiochem, La Jolla, CA, USA)], 60 ml buffer A. Elution of subunit I with buffer B was detected as o.1 unit absorbance raise at 280 nm caused by the detergent Zwittergent 3–12. Fractions containing subunit I were concentrated with Centriprep 30 kDa concentrators (Millipore Corporation, Bedford, MA, USA).

Subunit II—Recombinant spinach subunit II with a slightly modified N-terminus was expressed in *E. coli* and purified as described by Tiburzy *et al*. (*17*). The N-terminus of the expressed subunit II reads ARIDEIEK instead of EEIEK of the bona fide subunit II.

Protein Analysis—SDS–PAGE, Coomassie Brillant Blue R-250 staining and protein determination were performed as described (*35*). Staining with silver nitrate was conducted to reveal impurities (*36*). When determining the N-terminal protein sequence of subunit I, SDS–PAGE with borate buffer according to Poduslo (*37*) was employed.

For sequencing, proteins were transferred after borate SDS–PAGE to PVDF membranes (Bio-Rad Laboratories, Hercules, CA, USA) with a Bio-Rad transfer device Trans-Blot SD using the 'semi-dry' technique (*38*). Membranes were stained with 0.1% (w/v) Coomassie

R-250 in 50% (v/v) methanol and bands cut out with a scalpel. N-terminal sequencing was carried out by automated Edman degradation.

CD Spectroscopy—CD spectra of 0.19 mg/ml subunit I were recorded in buffer B (10 mM Tricine/NaOH pH 7.8, 5 mM DTT, 20 mM Zwittergent 3–12) with a Jasco J-720 CD spectrometer (JASCO Inc., Easton, MD, USA) at 4°C and a cuvette of 0.1 mm path length. The spectra were acquired at a resolution of 0.5 nm, 1 nm band width, 20 mdeg sensitivity, 1 s response time, 50 nm/min scanning speed.

To record the CD spectra of subunit II, 0.1 mg/ml subunit II in 10 mM Tricine/NaOH pH 7.8 with or without 20 mM Zwittergent 3–12, a Jasco J-715 CD spectrometer (JASCO Inc., Easton, MD, USA) at 4°C and a cuvette of 1 mm path length was employed. The secondary structure of subunits I and II was analysed by the software CDNN v2.1 (*39*).

FTIR Spectroscopy—Subunit I was concentrated with Centricon 30 kDa concentrators (Millipore Corporation, Bedford, MA, USA) while the solvent was changed to buffer B (10 mM Tricine/NaOH pH 7.8, 5 mM DTT, 20 mM Zwittergent 3–12) with D_2O as solvent. Subunit II was measured in 10 mM phosphate buffer pH 7.5 with D_2O as solvent. Measurements were performed on a Bruker Vector 22 (Bruker Optics, Ettlingen, Germany) at RT. The sample has been prepared on a CaF_2 cuvette with 10 μm path length. A sum of Gaussians were used to fit the amide I′ band of the recorded IR spectrum [for more details see Poetsch *et al*. (*40*)].

RESULTS

Secondary Structure Prediction—In contrast to eubacteria, chloroplast ATP synthases possess two different peripheral stalk subunits. At first bioinformatics analysis was carried out to verify if the low sequence similarity leads to different predicted structures of the subunits I and II.

Subunits I and II from spinach chloroplast were aligned to the sequence of subunit b from *E. coli* according to Tiburzy and Berzborn (*17*). Different algorithms were employed to predict the secondary structure of the subunits (Fig. 1). For this figure, we have limited the sequence of subunit II to the mature peptide chain which are the amino acids 76–222. The N-terminal part of the subunits I and II is predicted to be unordered; this part is longer for subunit II. The next part is the transmembrane helix. The starting point of the helix is predicted for the subunits I and II at the same position in the alignment with b from *E. coli* (Ala5). In the structure of the transmembrane domain of *E. coli* b (*18*), the start of the transmembrane helix is at Asn4. This NMR structure in organic solvents (*18*) shows a bend in the helix from residues 23 to 26. Our analysis predicts an interception for subunit II in this region, which can be interpreted also as a bend. The presence of a bend is less obvious for subunit I, since it is only predicted by PHD. On the sequence level, the proline at position 28 in *E. coli* b is conserved in spinach II but mutated to a glycine in spinach I. The tether and dimerization domains (residues 24–122 in *E. coli* b) are predicted to be helical for both subunits I and II. The C-terminal part of the subunit b (residues 123–156) from *E. coli* interacts with the subunit δ (*41*). It has been demonstrated by chemical crosslinking that the four last C-terminal amino acids of the subunit I from CF_OF_1 interact with the subunit δ (*42*), too. In the alignment, the C-terminus of subunit I is nine residues longer than in *E. coli* subunit b. Our analysis predicts an interception of a helix from residues 142 to 145 for subunit I, which may represent a flexible region or an additional bend. This region is followed by a short helical segment of about 16 residues. The flexible region and the helix were also predicted for subunit b from *E. coli* (data not shown). The sequence of subunit II is shorter and ends in the alignment before the start of this segment. At the C-terminus, the last four residues of subunit II and the last six residues of subunit I are predicted to be unstructured. This is in contrast to the subunit b from *E. coli*, where the last 10 residues are predicted to form a helix (*43*).

Coiled–coil Prediction—For eubacteria and mitochondria biochemical and bioinformatics data describe coiled–coil interactions of the subunit b (*11*, *12*). Although this can also be expected for the chloroplast subunits I and II, no report has been published, so far.

Three different programs were used for the prediction of coiled–coil regions in the subunits I (b) and II (b′) (Fig. 2). As organisms, six Viridiplantae (*S. oleracea*, *O. sativa*, *A. thaliana*, *C. reinhardtii*, *C. vulgaris* and *Volvox calteri f. nagariensis*), two Cyanobacteria (*Thermosynechococcus elongatus BP-1* and *Synechocystis sp. PCC 6803*) and one from Glaucocystophyceae (*C. paradoxa*), Cryptophyta (*G. theta*) and Proteobacteria (*E. coli*) were selected. For Fig. 2 only organisms with distinct differences in the prediction are shown (see legend). For *S. oleracea* and *C. reinhardtii*, subunit II includes the transition peptide sequences in agreement with the seqences in the database. Only the mature chain of spinach is known (amino acids 76–222). Coils and Paircoil (Paircoil: in addition pair-wise correlation scores) use position-specific scoring matrices for the prediction of coiled–coil regions, whereas Marcoil uses a hidden Markov model. Coils uses the simplest algorithm of all three programs and is probably the least exact. We first investigated, whether there are general differences between the three programs. For all sequences except subunit II from *C. reinhardtii*, Paircoil often calculates a lower coiled–coil probability per residue. Often smoother profiles are computed by Marcoil in comparison to Coils and Paircoil. If the probability cut-off for coiled–coil regions is set to 0.5, the predicted dimerization domain of subunit b from *E. coli* extends from residues ~40 to ~130. This is in good agreement with the experimentally determined dimerization region from Asp53 to Lys122 (*44*). Out of all three algorithms, the Paircoil prediction was closest to the experimental data from *E. coli* b. However, we doubt that one example is sufficient to conclude that Paircoil is the best algorithm in general. Indeed, it was noticed previously that the pair-wise correlation scores are often too strict due to the limited training dataset, which explains the overall lowest probability scores (*28*). For both subunits b and b′ from

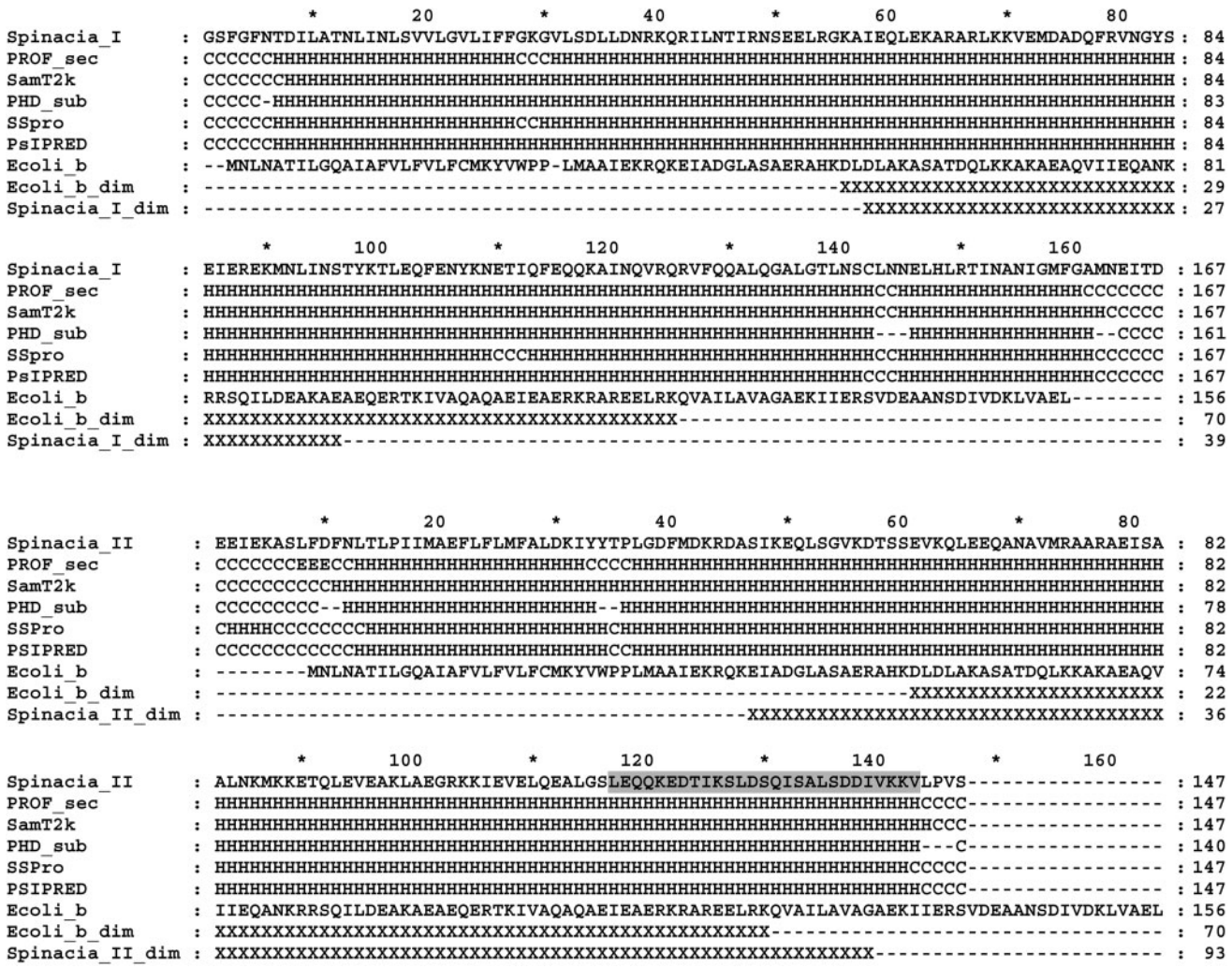

Fig. 1. **Secondary structure prediction for the mature subunits I and II from spinach chloroplast.** PROF_sec: prediction from PHD with multiple sequence alignment as input, PHD_sub subset (>82% accuracy) from PHD with single sequence as input. 'H' are α-helical regions and 'C' random coils. Coiled–coil regions are marked with 'X'. For *E. coli*, the experimentally determined region is shown. The predicted regions from the subunits I and II are marked with 'X', if the mean probability from the three coiled–coil prediction programs is >0.5. Amphipathic helix windings are grey shaded.

the two cyanobacteria, coiled–coil regions of ~100 residues are predicted. Except *Chlorella vulgaris*, shorter regions are predicted for subunit I from chloroplasts. The length of the regions decreases from ~90 residues for *Cyanophora paradoxa*, ~60 residues for *Chlamydomonas reinhardtii* to only ~40 residues for subunit I from spinach, rice and *arabidopsis*. This very small region supports the uniqueness of subunit I. The subunits II from higher plants all contain a coiled–coil region of ~100 residues, similar to subunit b in *E. coli*. Low probabilities of forming coiled–coils are calculated by all programs for subunit II from *C. reinhardtii* and *Volvox*. For the two organisms, the programs predicted only short regions with a probability above 0.5.

Isolation of Subunit I—To achieve unambiguous results in CD and FTIR measurements it is of utmost importance to have a very pure protein sample. Although a procedure published in 1990 should allow isolating subunits of CF_O (*45*, *46*), it does not separate them completely. When we applied the procedure, subunit I was contaminated with subunits III and IV and additionally various other proteins. The purity of such sample was not sufficient for spectroscopy. Therefore, in previous years we have optimized the isolation procedure of subunit I leading to a very pure sample. For removal of non-ATP synthase proteins, dialyzed CF_OF_1 from the sucrose gradient with CHAPS as detergent was applied to the DEAE–Trisacryl column. By replacing phosphate in all buffers with tricine, we changed the elution order of ATP synthase subunits compared to (*45*).

During chromatography with the detergent-free buffer A, unbound protein was eluted at 50 and 80 ml (Fig. 3A). A steep raise in the UV absorption at 110 ml indicates the start of protein elution from the column with buffer B. The fractions eluted first contained besides the subunit I impurities with molecular masses of 43 and 27 kDa (Fig. 3B, lanes 1 and 2). Starting with ~140 ml

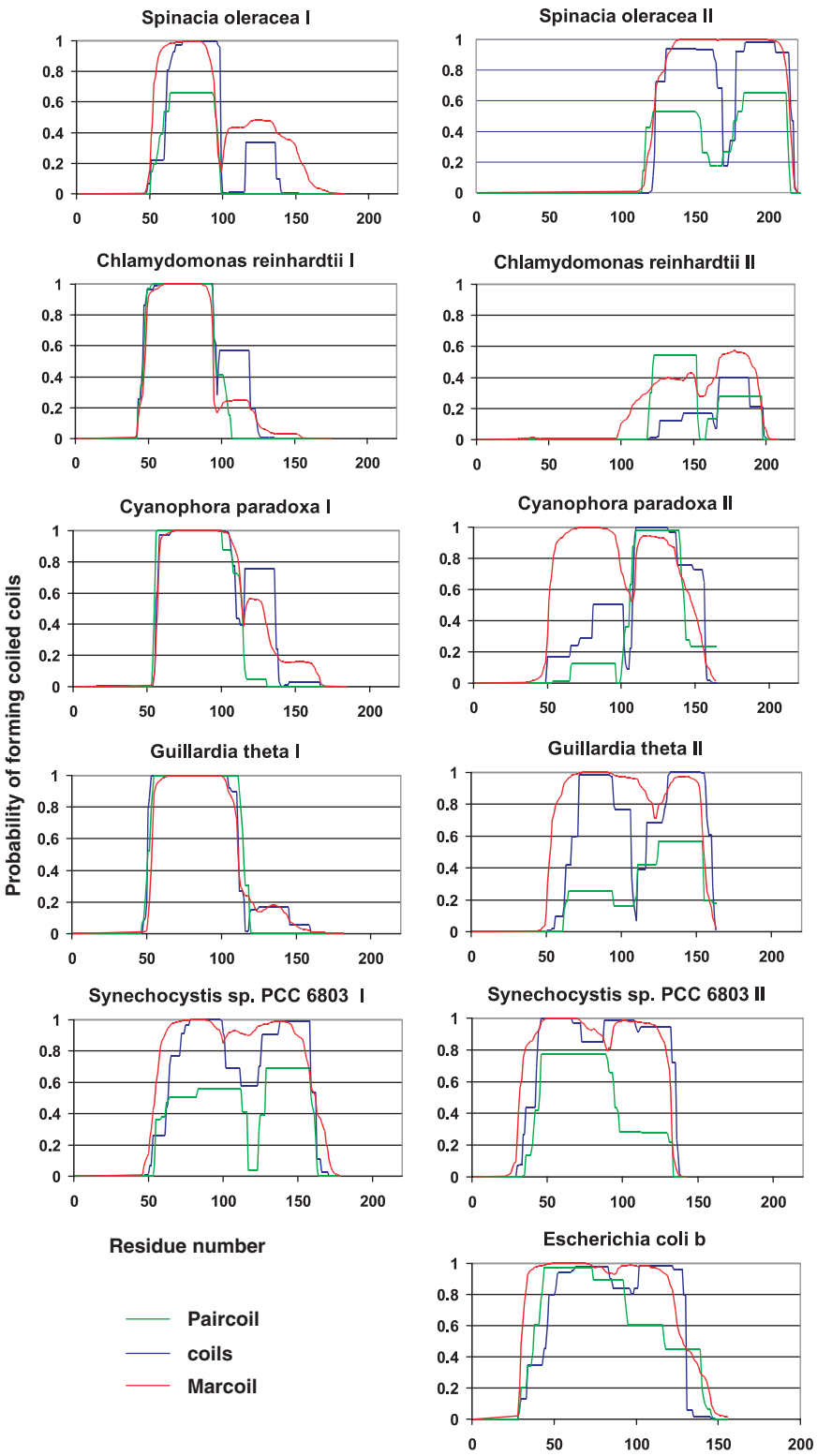

Fig. 2. **Probability of forming coiled–coils was predicted with the programs Coils, Paircoil and Marcoil for the subunits I (b) and II (b′).** Only organisms with distinct differences in the prediction are shown: Viridplantae: *S. oleracea* and *C. reinhardtii*, Glaucocystophyceae: *C. paradoxa*, Cryptophyta: *G. theta*, Cyanobacteria: *Synechocystis sp. PCC 6803* and Proteobacteria: *Escherichia coli*. The sequences of *S. oleracea* and *C. reinhardtii* subunit II are presented as deposited in the databases including the transition peptides (in spinach mature chain from 76 to 222).

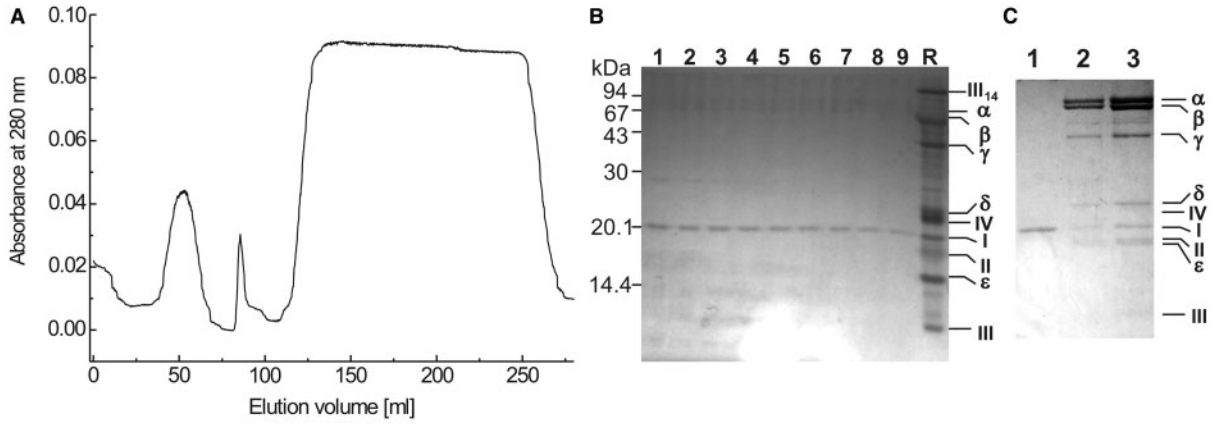

Fig. 3. **Isolation of subunit I.** A: Chromatography using DEAE–Trisacryl was performed to isolate the subunit I, flow rate 1 ml/min, 4°C. Subunit I is eluted in the volume 110 to 275 ml by a buffer (10 mM Tricine/NaOH pH 7.8, 5 mM DTT) containing the detergent Zwittergent 3–12 (20 mM). B: Proteins were separated by SDS–PAGE (T = 14%, C = 4%). To analyse the purity of the eluted fractions, the gel was silver stained. Lanes 1–9: chromatography fractions from 120 to 260 ml, lane R: 6 μg purified CF_OF_1. C: Proteins were separated by SDS–PAGE (T = 14%, C = 4%). To analyse the pooled fractions containing subunit I (elution volume 140–275 ml), the gel was stained with Coomassie R-250. Lane 1: eluted subunit I, lane 2: 2 μg CF_OF_1, lane 3: 4 μg CF_OF_1.

only the subunit I was detected in the eluted fractions (lanes 3–9 in Fig. 3B). The purest fractions eluting from 140 to 275 ml containing only subunit I according to SDS–PAGE were pooled and concentrated with Centriprep 30 kDa. Although subunit I has a molecular mass of 19 kDa only, in the presence of detergent it was retained completely by the membrane of the Centriprep concentrator. The concentrate was analysed by SDS–PAGE and Coomassie staining (Fig. 3C, lane 1). Only one protein band was stained, which migrated to the same position as the subunit I from the CF_OF_1 reference. N-terminal sequencing was carried out to verify that the isolated protein is indeed the subunit I. The sequence of the first 10 amino acids (GSFGFNTDIL) of the isolated protein was identical to subunit I of CF_OF_1 from *Spinacia oleracea*. The purest eluted fractions contained 20% of the subunit I present in the dialysed CF_OF_1, resulting in 0.3 mg pure subunit I from 40 mg CF_OF_1.

Secondary Structure of Subunit I—The CD spectrum of subunit I was recorded in buffer B. The CD spectrum (Fig. 4A) of subunit I shows a double minimum at 208 and 222 nm, indicating that the predominant structural element of subunit I is the α-helix. The contribution of each protein secondary structure element to the spectrum was quantified by the CDNN algorithm (Table 1).

To measure the FTIR spectrum, H_2O was replaced by D_2O. The FTIR spectrum of the subunit I (Fig. 4B) has two absorption bands at 1735 and 1650 cm^{-1}. The absorption band at 1735 cm^{-1} is caused by the C=O stretch of the ester group of the lipids. This reveals that residual lipid—most likely asolectin in the gradient buffer of the CF_OF_1 isolation—is present in the sample. The amide I absorption band of the peptide bond (C=O stretching vibration in D_2O) at 1650 cm^{-1} was fitted by Gauss functions to calculate the proportion of each secondary structure element (Table 1). It is evident that the α-helix is the predominant structural element. The determination of the other secondary structure elements fairly agrees with the content as determined by CD (Table 1). It can be stated that CD spectroscopy leads generally to a higher proportion of the α-helical content, whereas FTIR overestimates the β-sheet content. This phenomenon is related to the different sensitivity of the selected spectroscopic technique for the respective structural element.

Secondary Structure of Subunit II—The CD spectrum of subunit II was recorded in 10 mM Tricine buffer pH 7.8 with or without 20 mM Zwittergent 3–12. Since the protein is expressed in soluble form in *E. coli* (*47*), we also measured a CD spectrum and the FTIR spectrum in the absence of detergent. The CD spectrum (Fig. 5A) of the subunit II in detergent shows a double minimum at 208 and 222 nm with a more pronounced minimum at 208 nm. Additionally, the value of the maximum at 190 nm is not 3-fold the absolute value of the minima, indicating that other secondary structure elements are strongly contributing in subunit II. After quantifying the contribution of each protein secondary structure element to the spectrum by the CDNN algorithm (Table 1), it is obvious, that helix and random coil contribute each to one-third to the total content of all structure elements for subunit II without detergent, and that the α-helical content increases and the random coil content decreases after detergent addition. Whereas for the proportion of α-helix the CD and FTIR data agree, the proportion of 41% β-sheet determined from FTIR without added detergent is much higher than the 18% from CD for reason as described earlier.

DISCUSSION

While the structures of F_1 subunits are determined up to high resolution, much less is known about the subunits of the membrane integral F_O part of the ATP synthase. In case of homologous subunits, structural information

from other organisms could be assigned to the chloroplast ATP synthase. However, subunit I is unique for chloroplasts (*17*). Additionally, no biochemical and structural information concerning subunits I and II were available.

In 1990 a chromatographic method for isolation of CF_O subunits was developed by Feng and McCarty (*45*, *46*). Unfortunately, this method using the detergent Zwittergent 3–12 and a DEAE Trisacryl column is not able to provide really pure subunit I (as described in Results section). One disadvantage is the starting material (ammonium sulphate precipitate), which leads to contamination with various proteins of unknown identity. In our procedure, this problem was solved by

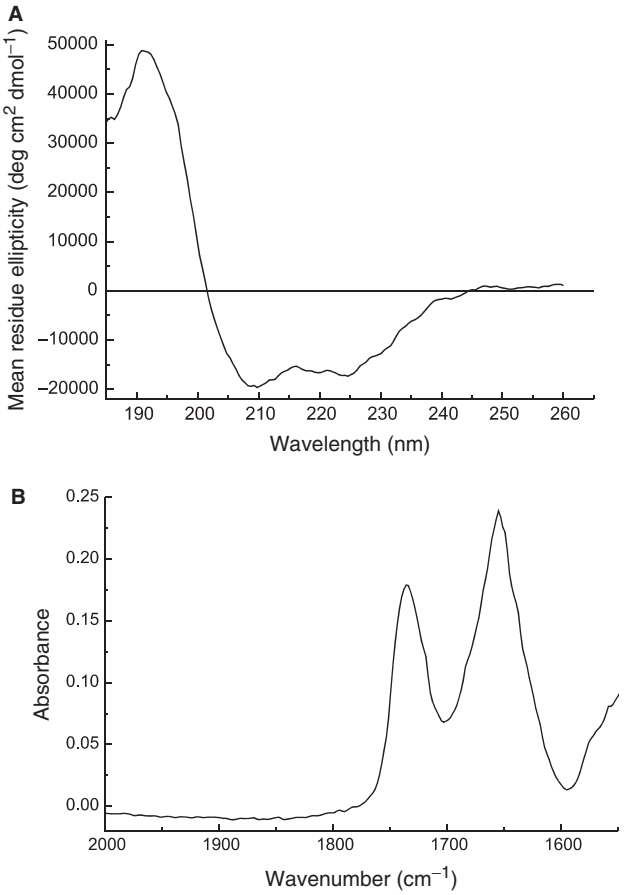

Fig. 4. **Spectra of isolated subunit I.** A: Subunit I (0.19 mg/ml in 10 mM Tricine/NaOH pH 7.8, 5 mM DTT, 20 mM Zwittergent 3–12) was isolated by DEAE-chromatography as described. The CD spectrum was acquired by averaging five single spectra and conversion into mean residue ellipticity. B: FTIR spectrum of subunit I in D_2O. Only the range around the relevant amide I vibration (1650 cm^{-1}) is depicted. The band at 1735 cm^{-1} is due to the lipid ester group. Contributions of the solvent have been subtracted.

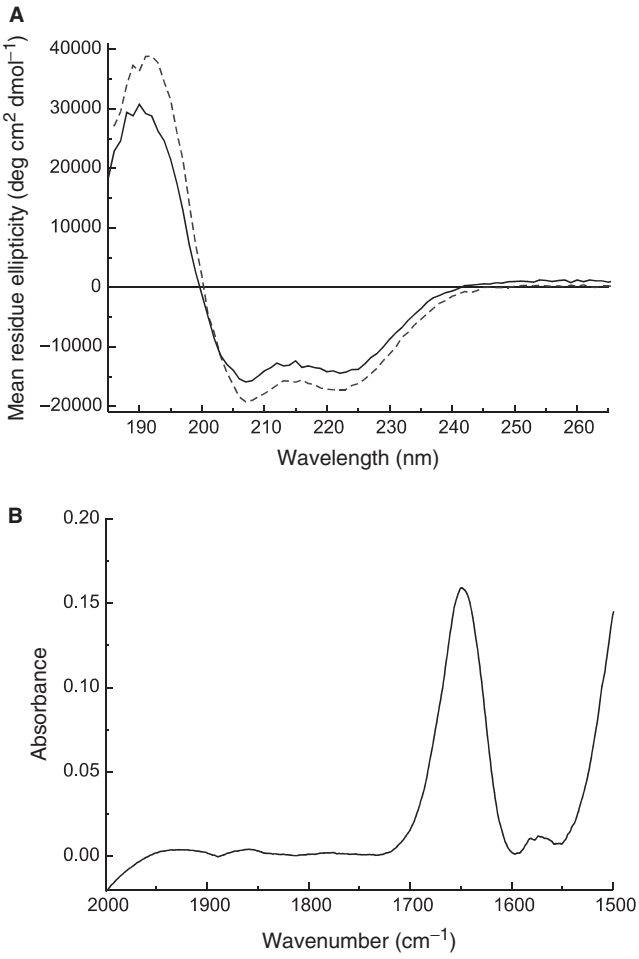

Fig. 5. **Spectra of isolated subunit II.** A: Subunit II (0.1 mg/ml in 10 mM Tricine/NaOH pH 7.8) was measured in the presence (dashed line) or absence of 20 mM Zwittergent 3–12 (solid line). The CD spectrum was acquired by averaging five single spectra and conversion into mean residue ellipticity. B: FTIR spectrum of subunit II in the amide I′ region in the absence of Zwittergent. Solvent contributions have been subtracted.

Table 1. **Secondary structure elements.**

Secondary structure element[a]	Subunit I		Subunit II		
	Proportion in % from CD	Proportion in % from FTIR	Proportion in % from CD		Proportion in % from FTIR without Zwittergent 3–12
			With Zwittergent 3–12	Without Zwittergent 3–12	
α-Helix	67	57	41	33	30
β-Pleated sheet	4	7	12	18	41
Random coil	14	23	25	30	8
Turn	12	13	16	16	21

[a]Proportion of each structural element as calculated by the software CDNN v2.1 (*39*) for the CD spectra and fitting with Gaussians for FTIR.

using a purified ATP synthase preparation instead of a crude ammonium sulphate precipitate. Another problem was contamination of subunit I with subunits III and IV. An elution profile in (*45*) illustrates that subunit IV elutes before a mixture of I, III and IV, and the last fractions contain only subunit I. In our hands, subunit I was contaminated with III and IV in all fractions. A critical point was the choice of buffer. By using phosphate buffer according to (*45*) the subunits III and IV were present. We have screened various buffers and observed that by replacing phosphate with tricine the elution order of ATP synthase subunits changes. Now, only subunit I elutes from the column.

Our mild procedure yielded subunit I in the presence of the detergent Zwittergent 3–12 in high purity and amounts sufficient for spectroscopy (CD and FTIR) but not for high-resolution techniques like NMR or 3D crystallization. CD and FTIR revealed that the α-helix is the predominant structural element in subunit I. However, the proportion of 67% (CD)/57% (FTIR) for chloroplasts is less than the published value of 80% with CD spectroscopy for *E. coli* subunit b reconstituted in lipid vesicles (*48*). Certainly, the surrounding of the proteins influences the α-helix proportion considerably. Greie *et al*. (*48*) also reported a proportion of 70% when they measured *E. coli* subunit b in detergent which is much closer to our values for subunit I. The different proportion of α-helix may reflect different interactions of the protein with their native membrane environment compared to the detergent micelle. Subunit II displayed a much smaller proportion of α-helix and a higher proportion of random coil than subunit I in the presence of detergent. The helical content was even lower and the random coil content higher in the absence of detergent. This observation in combination with the substantial content of random coil and loops indicates a high flexibility of subunit II. Low helical contents of 45% determined with CD spectroscopy for the cytoplasmic domain of subunit b and 39% for subunit b′ were reported previously for the cyanobacterial ATP synthase (*15*). Therefore, it can be speculated that this difference in helix content is an essential feature of photosynthetic ATP synthases but not of *E. coli*. Upon combining both subunits the helical content increased to 58%, which is still ~20% lower than the value of the homodimer from *E. coli* (*48*).

The dramatic increase of sequence information and the improvement of sequence analysis software during recent years motivated us to re-examine subunits I and II by bioinformatics tools. In contrast to the subunit b from *E. coli*, structural and functional information about the subunits I and II of chloroplasts are still scarce. Our secondary structure prediction of the subunits I and II revealed that both are mainly α-helical. The predicted proportion of α-helix is 92% for subunit I and 88% for subunit II. These predictions are for subunit I significantly higher and for subunit II much higher than the values obtained from spectroscopy. The rather large discrepancy between the measured and the predicted helical content of subunits I and II may be due to the high flexibility of single b-type subunits. Recent secondary structure predictions identified a turn region at residue 79–85 in *E. coli* b (*49*), but its existence was doubted based on experimental results (*12*). When we reanalysed the *E. coli* b sequence, no turn in this region was predicted by the software used in our study (data no shown)—an indication for the improvement of prediction software. The opinion that subunit I is functionally equivalent to subunit b from eubacteria has been challenged by a bioinformatics analysis from Tiburzy and Berzborn (*17*). One example is the region around proline 28 in *E. coli* which is conserved in subunit II but mutated in subunit I to glycine and followed by a valine residue being out of the sequence alignment (Fig. 1). Therefore, subunit I should possess an increased local conformational flexibility in this region. Subunit I possess a helical segment at the C-terminus which is embedded between two flexible regions. This segment is absent in the shorter subunit II and probably plays a role in the binding to δ and may also bind to α, since for *E. coli* a b-α crosslink was detected in this region (*20*). Since up to now no strong experimental evidence for an interaction of subunit II with δ or other subunits from CF_1 could be obtained and experiments from *E. coli* show that a deletion of the last four C-terminal residues of one subunit b in a heterodimer is functionally tolerated, it is plausible that no interaction between II and δ exists (*50*).

To further examine, whether structural differences exist between the subunits I and II, a coiled–coil prediction was carried out using the three different programs Coils, Paircoil and Marcoil. For subunit I, a much shorter coiled–coiled region was predicted than for subunit II. In face of the experimentally determined α-helical content of both subunits, it must be asked to which extent theoretical and experimental values agree. An α-helical content of about 62% for subunit I does not exclude the possibility of an about 50 amino acids long coiled–coiled region. For the smaller subunit II, an about 100 amino acids long coiled–coil region was predicted, yet the measured α-helical content is only between 30 and 41%. Since 100 amino acids comprise about 68% of the sequence, the predicted length of the coiled–coil region is inconsistent with the experimental data. While such a long coiled–coil region appears to be absent in the isolated subunit II, it may still be possible that a longer coiled–coil region exists in the holoenzyme. This speculation is supported by the observed high flexibility in subunit II and the reported conformational changes upon heterodimerization of cyanobacterial b and b′ (*15*).

In the alignment of 51 b-type ATP synthase subunits a strictly conserved Arg is obviously close to the hydrophobic membrane spanning residues (*17*). It is located in a conserved hydrophobic face of an amphipathic heptade pattern, suggesting four helix windings: h x x x h x x R x x x h x x x h (h = hydrophobic residue), in spinach II: LGDFMDK(R44)DASI. Although it may imply that the positive charge of arginine is needed twice in all homodimeric or heterodimeric ATP synthase subunit b pairs (*17*), Grabar and Cain (*50*) showed for *E. coli* that the deletion of one Arg residue per heterodimer only leads to an impairment of activity, but not a complete loss of function. All newly published homologous sequences analysed by us now display this 'signature', too.

At the C-terminal part of spinach CF_oII a unique feature was discovered, consisting of seven amphipathic helix windings with two conserved positive charges

embedded in the putative hydrophobic face (grey shaded region in Fig. 1). When comparing the sequences of several organisms, additional positive charged amino acids can be identified but two (K121 and K142 in spinach CF_oII) are conserved. The heptade pattern in the primary sequence suggests that the two positive charges would be placed within a coiled coil at a distance of about 30 Å. This feature was strongly conserved among all eubacterial subunits F_ob and all subunits b̀ and CF_oII of photosynthetic organisms, but lost in subunits CF_oI and F_ob of photosynthetic organisms (*17*) and in the subunits CF_OII from *Volvox* and *Chlamydomonas*. However, a homologous pattern seems to have evolved in the C-terminal region of *Chlamydomonas* CF_oI. (The sequence of *Volvox* CF_oI is not yet available.) The functional relevance of the two (sometimes three) positive charges within the conserved hydrophobic face, i.e. within the interaction contacts of the putative coil, is still unknown.

So far, there have not been many efforts to better understand the structural and functional role of the subunits I and II from plants in relation to subunit b from eubacteria. As already pointed out by Tiburzy and Berzborn (*17*), it still remains to be shown, whether subunits I or II can complement the function of subunit b in the bacterial enzyme, since former experiments failed to come to a clear conclusion (*51*) or were retracted (*52*).

Concerning the degree of functional equivalence of subunits b and b′ in photosynthetic bacteria, it has to be tested whether it is possible to delete subunit b completely or in parts without impairing the function of the ATP synthase. Photoautotrophic growth of the cyanobacterium *Synechocystis PCC 6803* was unimpaired if the subunit b′ was truncated down to the hydrophobic stretch but did not occur if its gene was deleted completely (*53*).

In *E. coli* each of the b subunits in the homodimer binds to different regions of F_1, thus interacting with it in an asymmetric manner, whereas two mutant b subunits can complement resulting in an intact ATP synthase (*50*). As conclusion, our results support the assumption that the photosynthetic organisms developed two different subunits as a better adaption to the different interaction sites (*15*, *54*).

We sincerely thank Dr J. Tiburzy and R. Oworah-Nkruma, Department of Biochemistry of Plants, Ruhr-University-Bochum, D-44780 Bochum, Germany, for providing heterologously expressed subunit II.
This work was supported by the Deutsche Forschungsgemeinschaft (Sonderforschungsbereich 472, to N.A.D. and H.S.).

REFERENCES

1. Böttcher, B., Schwarz, L., and Gräber, P. (1998) Direct indication for the existence of a double stalk in CF_OF_1. *J. Mol. Biol.* **281**, 757–762
2. Stock, D., Leslie, A.G., and Walker, J.E. (1999) Molecular architecture of the rotary motor in ATP synthase. *Science* **286**, 1700–1705
3. Meier, T., Polzer, P., Diederichs, K., Welte, W., and Dimroth, P. (2005) Structure of the rotor ring of F-Type Na^+-ATPase from *Ilyobacter tartaricus*. *Science* **308**, 659–662
4. Murata, T., Yamato, I., Kakinuma, Y., Leslie, A.G., and Walker, J.E. (2005) Structure of the rotor of the V-Type Na^+-ATPase from *Enterococcus hirae*. *Science* **308**, 654–659
5. Seelert, H., Poetsch, A., Dencher, N.A., Engel, A., Stahlberg, H., and Müller, D.J. (2000) Structural biology. Proton-powered turbine of a plant motor. *Nature* **405**, 418–419
6. Stahlberg, H., Müller, D.J., Suda, K., Fotiadis, D., Engel, A., Meier, T., Matthey, U., and Dimroth, P. (2001) Bacterial Na^+-ATP synthase has an undecameric rotor. *EMBO Rep.* **2**, 229–233
7. Rastogi, V.K. and Girvin, M.E. (1999) Structural changes linked to proton translocation by subunit c of the ATP synthase. *Nature* **402**, 263–268
8. Wilkens, S., Zhou, J., Nakayama, R., Dunn, S.D., and Capaldi, R.A. (2000) Localization of the δ subunit in the *Escherichia coli* F_1F_O-ATPsynthase by immuno electron microscopy: the δ subunit binds on top of the F_1. *J. Mol. Biol.* **295**, 387–391
9. Rodgers, A.J., Wilkens, S., Aggeler, R., Morris, M.B., Howitt, S.M., and Capaldi, R.A. (1997) The subunit δ-subunit b domain of the *Escherichia coli* F_1F_O ATPase. The b subunits interact with F_1 as a dimer and through the δ subunit. *J. Biol. Chem.* **272**, 31058–31064
10. McLachlin, D.T. and Dunn, S.D. (1997) Dimerization interactions of the *b* subunit of the *Escherichia coli* F_1F_O-ATPase. *J. Biol. Chem.* **272**, 21233–21239
11. Hong, S. and Pedersen, P.L. (2003) ATP synthases: insights into their motor functions from sequence and structural analyses. *J. Bioenerg. Biomembr.* **35**, 95–120
12. Del Rizzo, P.A., Bi, Y., Dunn, S.D., and Shilton, B.H. (2002) The "second stalk" of *Escherichia coli* ATP synthase: structure of the isolated dimerization domain. *Biochemistry* **41**, 6875–6884
13. Dunn, S.D., Revington, M., Cipriano, D.J., and Shilton, B.H. (2000) The *b* subunit of *Escherichia coli* ATP synthase. *J. Bioenerg. Biomembr.* **32**, 347–355
14. Dickson, V.K., Silvester, J.A., Fearnley, I.M., Leslie, A.G., and Walker, J.E. (2006) On the structure of the stator of the mitochondrial ATP synthase. *EMBO J.* **25**, 2911–2918
15. Dunn, S.D., Kellner, E., and Lill, H. (2001) Specific heterodimer formation by the cytoplasmic domains of the *b* and *b′* subunits of cyanobacterial ATP synthase. *Biochemistry* **40**, 187–192
16. Herrmann, R.G., Steppuhn, J., Herrmann, G.S., and Nelson, N. (1993) The nuclear-encoded polypeptide CF_O-II from spinach is a real, ninth subunit of chloroplast ATP synthase. *FEBS Lett.* **326**, 192–198
17. Tiburzy, H.J. and Berzborn, R.J. (1997) Subunit II (*b′*) and not subunit I (*b*) of photosynthetic ATP synthases is equivalent to subunit b of the ATP synthases from nonphotosynthetic eubacteria. Evidence for a new assignment of b-type F_O subunits. *Z. Naturforsch. [C]* **52**, 789–798
18. Dmitriev, O., Jones, P.C., Jiang, W., and Fillingame, R.H. (1999) Structure of the membrane domain of subunit *b* of the *Escherichia coli* F_OF_1 ATP synthase. *J. Biol. Chem.* **274**, 15598–15604
19. Dunn, S.D. (1992) The polar domain of the *b* subunit of *Escherichia coli* F_1F_O-ATPase forms an elongated dimer that interacts with the F_1 sector. *J. Biol. Chem.* **267**, 7630–7636
20. Rodgers, A.J. and Capaldi, R.A. (1998) The second stalk composed of the *b*- and δ-subunits connects F_O to F_1 via an α-subunit in the *Escherichia coli* ATP synthase. *J. Biol. Chem.* **273**, 29406–29410
21. Weber, J., Wilke-Mounts, S., Nadanaciva, S., and Senior, A.E. (2004) Quantitative determination of direct binding of *b* subunit to F_1 in *Escherichia coli* F_1F_0-ATP synthase. *J. Biol. Chem.* **279**, 11253–11258

22. Sorgen, P.L., Caviston, T.L., Perry, R.C., and Cain, B.D. (1998) Deletions in the second stalk of F_1F_O-ATP synthase in *Escherichia coli*. *J. Biol. Chem.* **273**, 27873–27878
23. Sorgen, P.L., Bubb, M.R., and Cain, B.D. (1999) Lengthening the second stalk of F_1F_O ATP synthase in *Escherichia coli*. *J. Biol. Chem.* **274**, 36261–36266
24. Grabar, T.B. and Cain, B.D. (2003) Integration of b subunits of unequal lengths into F_1F_0-ATP synthase. *J. Biol. Chem.* **278**, 34751–34756
25. Altschul, S.F., Madden, T.L., Schaffer, A.A., Zhang, J., Zhang, Z., Miller, W., and Lipman, D.J. (1997) Gapped BLAST and PSI-BLAST: a new generation of protein database search programs. *Nucleic Acids Res.* **25**, 3389–3402
26. Lupas, A., Van Dyke, M., and Stock, J. (1991) Predicting coiled coils from protein sequences. *Science* **252**, 1162–1164
27. Berger, B., Wilson, D.B., Wolf, E., Tonchev, T., Milla, M., and Kim, P.S. (1995) Predicting coiled coils by use of pairwise residue correlations. *Proc. Natl. Acad. Sci. U.S.A.* **92**, 8259–8263
28. Delorenzi, M. and Speed, T. (2002) An HMM model for coiled-coil domains and a comparison with PSSM-based predictions. *Bioinformatics* **18**, 617–625
29. Rost, B. and Sander, C. (1994) Combining evolutionary information and neural networks to predict protein secondary structure. *Proteins* **19**, 55–72
30. Karplus, K., Karchin, R., Draper, J., Casper, J., Mandel-Gutfreund, Y., Diekhans, M., and Hughey, R. (2003) Combining local-structure, fold-recognition, and new-fold methods for protein structure prediction. *Proteins* **53**(Suppl 6), 491–496
31. Baldi, P., Brunak, S., Frasconi, P., Soda, G., and Pollastri, G. (1999) Exploiting the past and the future in protein secondary structure prediction. *Bioinformatics* **15**, 937–946
32. Jones, D.T. (1999) Protein secondary structure prediction based on position-specific scoring matrices. *J. Mol. Biol.* **292**, 195–202
33. Fromme, P., Boekema, E.J., and Gräber, P. (1987) Isolation and characterization of a supramolecular complex of subunit III of the ATP synthase from chloroplasts. *Z. Naturforsch. [C]* **42c**, 1239–1245
34. Pick, U. and Racker, E. (1979) Purification and reconstitution of the N,N′-dicyclohexylcarbodiimide-sensitive ATPase complex from spinach chloroplasts. *J. Biol. Chem.* **254**, 2793–2799
35. Poetsch, A., Seelert, H., Meyer zu Tittingdorf, J., and Dencher, N.A. (1999) Detergent effect on anion exchange perfusion chromatography and gel filtration of intact chloroplast H^+-ATP synthase. *Biochem. Biophys. Res. Commun.* **265**, 520–524
36. Oakley, B.R., Kirsch, D.R., and Morris, N.R. (1980) A simplified ultrasensitive silver stain for detecting proteins in polyacrylamide gels. *Anal. Biochem.* **105**, 361–363
37. Poduslo, J.F. (1981) Glycoprotein molecular-weight estimation using sodium dodecyl sulfate-pore gradient electrophoresis: comparison of tris-glycine and tris-borate-EDTA buffer systems. *Anal. Biochem.* **114**, 131–139
38. Kyhse-Andersen, J. (1984) Electroblotting of multiple gels: a simple apparatus without buffer tank for rapid transfer of proteins from polyacrylamide to nitrocellulose. *J. Biochem. Biophys. Methods* **10**, 203–209
39. Böhm, G., Muhr, R., and Jaenicke, R. (1992) Quantitative analysis of protein far UV circular dichroism spectra by neural networks. *Protein Eng.* **5**, 191–195
40. Poetsch, A., Rexroth, S., Heberle, J., Link, T.A., Dencher, N.A., and Seelert, H. (2003) Characterisation of subunit III and its oligomer from spinach chloroplast ATP synthase. *Biochim. Biophys. Acta* **1618**, 59–66
41. McLachlin, D.T., Bestard, J.A., and Dunn, S.D. (1998) The b and delta subunits of the *Escherichia coli* ATP synthase interact via residues in their C-terminal regions. *J. Biol. Chem.* **273**, 15162–15168
42. Beckers, G., Berzborn, R.J., and Strotmann, H. (1992) Zero-length crosslinking between subunits δ and I of the H^+-translocating ATPase of chloroplasts. *Biochim. Biophys. Acta* **1101**, 97–104
43. Dunn, S.D., McLachlin, D.T., and Revington, M. (2000) The second stalk of *Escherichia coli* ATP synthase. *Biochim. Biophys. Acta* **1458**, 356–363
44. Revington, M., McLachlin, D.T., Shaw, G.S., and Dunn, S.D. (1999) The dimerization domain of the *b* subunit of the *Escherichia coli* F_1F_O-ATPase. *J. Biol. Chem.* **274**, 31094–31101
45. Feng, Y. and McCarty, R.E. (1990) Chromatographic purification of the chloroplast ATP synthase (CF_O-CF_1) and the role of CF_O subunit IV in proton conduction. *J. Biol. Chem.* **265**, 12474–12480
46. Feng, Y. and McCarty, R.E. (1990) Subunit interactions within the chloroplast ATP synthase (CF_O-CF_1) as deduced by specific depletion of CF_O polypeptides. *J. Biol. Chem.* **265**, 12481–12485
47. Tiburzy, H.J., Zimmermann, M., Oworah-Nkruma, R., and Berzborn, R.J. (1999) *Z Naturforsch [C]* Vol. 54, pp. 230–238
48. Greie, J.C., Deckers-Hebestreit, G., and Altendorf, K. (2000) Secondary structure composition of reconstituted subunit *b* of the *Escherichia coli* ATP synthase. *Eur. J. Biochem.* **267**, 3040–3048
49. Revington, M., Dunn, S.D., and Shaw, G.S. (2002) Folding and stability of the b subunit of the F_1F_O ATP synthase. *Protein Sci.* **11**, 1227–1238
50. Grabar, T.B. and Cain, B.D. (2004) Genetic complementation between mutant *b* subunits in F_1F_0 ATP synthase. *J. Biol. Chem.* **279**, 31205–31211
51. Schmidt, G. (1992) Expression of subunit II of chloroplast H^+-ATPase in an *Escherichia coli* mutant lacking subunit b of its H^+-ATPase. *Acta Physiol. Scand. Suppl.* **607**, 275–278
52. Schmidt, G., Rodgers, A.J., Howitt, S.M., Munn, A.L., Hudson, G.S., Holten, T.A., Whitfeld, P.R., Bottomley, W., Gibson, F., and Cox, G.B. (1990) The chloroplast CF_OI subunit can replace the *b*-subunit of the F_OF_1-ATPase in a mutant strain of *Escherichia coli* K12. *Biochim. Biophys. Acta* **1015**, 195–199
53. Lill, H., Steinemann, D., and Nelson, N. (1994) Mutagenesis of the b′-subunit of *Synechocystis sp. PCC 6803* ATP-synthase. *Biochim. Biophys. Acta* **1184**, 284–290
54. Berzborn, R.J. (2000) *Probing Photosynthesis* (Yunus, M., Pathre, U., and Mohanty, P. eds) pp. 70–107 TAYLOR and Francis, London, New York